Intramolecular Electron Transfer in (BzImH)[$(LOV)_2O$] (H_2L = *S*-Methyl 3-((2-Hydroxyphenyl)methyl)dithiocarbazate): A Novel μ-Oxo Dinuclear Oxovanadium(IV/V) Compound with a Trapped-Valence $(V_2O_3)^{3+}$ Core

Subodh Kanti Dutta,[†] Sujit Baran Kumar,[†] Sudeep Bhattacharyya,[†] Edward R. T. Tiekink,[‡] and Muktimoy Chaudhury*[,†]

Department of Inorganic Chemistry, Indian Association for the Cultivation of Science, Calcutta 700 032, India, and Department of Chemistry, The University of Adelaide, Adelaide, South Australia 5005, Australia

Received January 30, 1997[⊗]

The mononuclear oxovanadium complexes [$V^{V}OL(OR)$] (R: Me, **1a**; Et, **1b**; Pr^{i}, **1c**) and [$V^{IV}OLB$] (B: Im, **2a**; BzIm, **2b**) of the tridentate ONS donor ligand *S*-methyl 3-((2-hydroxyphenyl)methyl)dithiocarbazate (H_2L) are reported. The novel mixed-valence (μ-oxo)divanadium(IV,V) complex (BzImH)[$(LVO)_2O$] (**3**) was synthesized using **1a** and **2b** as precursors. All of the complexes were characterized by various physical techniques, including ^{1}H NMR, EPR, and cyclic voltammetry. The X-ray structures of **1a** and **3** were determined. Crystals of **1a** are triclinic, of space group $P\bar{1}$, with $a = 11.045(1)$ Å, $b = 13.429(4)$ Å, $c = 9.611(1)$ Å, $\alpha = 100.00(1)°$, $\beta = 114.33(1)°$, $\gamma = 81.00(1)°$, and $Z = 4$. The asymmetric unit of **1a** contains two independent molecules with minor conformational differences. Crystals of **3** are monoclinic, of space group $P2_1/n$, with $a = 10.10(1)$ Å, $b = 20.594(9)$ Å, $c = 14.679(8)$ Å, $\beta = 95.28(6)°$, and $Z = 4$. **3** is a bent molecule, with a V−O−V bridge angle of 144.0(6)°. It has a trapped-valence structure in the solid state with a rare *syn*-dioxo−μ-oxo [OV−O−VO]$^{3+}$ core and reveals a 15-line EPR spectrum (^{51}V, $I = {}^7/_2$) in solution (CH_3CN) at room temperature, indicating delocalization of the odd electron. The spectrum gradually changes its profile with the lowering of temperature and ultimately collapses into an 8-line pattern at 225 K due to thermal trapping of the odd electron ($k_{th} \sim 7.3 \times 10^9$ s^{-1}). **3** also exhibits an intervalence transfer (IT) band in solution with features (λ_{max} 970 nm, ϵ 1670 M^{-1} cm^{-1} in CH_3CN) remaining practically unaffected by the change of solvents. The IT band was analyzed by Gaussian curve fitting, and the electron exchange integral H_{AB} was estimated as 2210 cm^{-1}. Thus, **3** appears to be an interesting mixed-oxidation-state (μ-oxo)divanadium(IV,V) complex that exhibits a trapped-valence structure in the solid state and undergoes valence delocalization in solution.

Introduction

The chemistry of vanadium is currently a subject of extensive research partly because of its increasingly recognized biochemical importance.[1−3] The distinct preference of this metal center for O- and/or N-coordination environments, as delineated by EXAFS[4] and crystallographic studies[5] on haloperoxidase, has prompted the synthesis of numerous model vanadium compounds containing O/N donor ligands, whose spectroscopic, magnetic, and redox properties have been widely investigated.[6−16] In contrast, vanadium/sulfur systems have so far received only limited attention[17−22] despite the reported involvement of such species in an alternative form of nitrogenase[23] and as an intermediates during the hydrosulfurization of crude oils.[24]

A prime objective of our research has been the synthesis and characterization of molybdenum complexes in biologically relevant oxidation states with the metal ion in a total or partial

[†] Indian Association for the Cultivation of Science.
[‡] The University of Adelaide.
[⊗] Abstract published in *Advance ACS Abstracts,* September 15, 1997.

(1) Chasteen, N. D. *Vanadium in Biological Systems*; Kluwer Academic Publishers: Dordrecht, The Netherlands, 1990.
(2) Butler, A.; Carrano, C. J. *Coord. Chem. Rev.* **1991**, *109*, 61.
(3) Rehder, D. *Angew. Chem., Int. Ed. Engl.* **1991**, *30*, 148.
(4) Arber, J. M.; deBoer, E.; Garner, C. D.; Hasnain, S. S.; Wever, R. *Biochemistry* **1989**, *28*, 7968.
(5) Messerschmidt, A.; Wever, R. *Proc. Natl. Acad. Sci. U.S.A.* **1996**, *93*, 392.
(6) Colpas, G. J.; Hamstra, B. J.; Kampf, J. W.; Pecoraro, V. L. *J. Am. Chem. Soc.* **1996**, *118*, 3469.
(7) Keramidas, A. D.; Papaioannou, A. B.; Vlahos, A.; Kabanos, T. A.; Bonas, G.; Makriyannis, A.; Rapropoulou, C. P.; Terzis, A. *Inorg. Chem.* **1996**, *35*, 357.
(8) Nanda, K. K.; Mohanta, S.; Ghosh, S.; Mukherjee, M.; Helliwell, M.; Nag, K. *Inorg. Chem.* **1995**, *34*, 2861.
(9) Cornman, C. R.; Zovinka, E. P.; Boyajian, Y. D.; Geiser-Bush, K. M.; Boyle, P. D.; Singh, P. *Inorg. Chem.* **1995**, *34*, 4213.
(10) Carrano, C. J.; Mohan, M.; Holmes, S. M.; de la Rosa, R.; Butler, A.; Charnock, J. M.; Garner, C. D. *Inorg. Chem.* **1994**, *33*, 646.
(11) Crans, D. C.; Shin, P. K. *J. Am. Chem. Soc.* **1994**, *116*, 1305.
(12) Armstrong, E. M.; Beddoes, R. L.; Calviou, L. J.; Charnock, J. M.; Collison, D.; Ertok, N.; Naismith, J. H.; Garner, C. D. *J. Am. Chem. Soc.* **1993**, *115*, 807.
(13) Clague, M. J.; Keder, N. L.; Butler, A. *Inorg. Chem.* **1993**, *32*, 4754.
(14) Vergopoulos, V.; Priebsch, W.; Fritzsche, M.; Rehder, D. *Inorg. Chem.* **1993**, *32*, 1844.
(15) Cornman, C. R.; Kampf, J.; Lah, M. S.; Pecoraro, V. L. *Inorg. Chem.* **1992**, *31*, 2035.
(16) Bulls, A. R.; Pippin, C. G.; Hahn, F. E.; Raymond, K. N. *J. Am. Chem. Soc.* **1990**, *112*, 2627.
(17) Klich, P. R.; Daniher, A. T.; Challen, P. R.; McConville, D. B.; Youngs, W. J. *Inorg. Chem.* **1996**, *35*, 347.
(18) Nanda, K. K.; Sinn, E.; Addison, A. W. *Inorg. Chem.* **1996**, *35*, 1.
(19) Reynolds, J. G.; Sendlinger, S. C.; Murray, A. M.; Huffman, J. C.; Christou, G. *Inorg. Chem.* **1995**, *34*, 5745.
(20) Henkel, G.; Krebs, B.; Schmidt, W. *Angew. Chem., Int. Ed. Engl.* **1992**, *31*, 1367.
(21) Heinrich, D. D.; Folting, K.; Huffman, J. C.; Reynolds, J. G.; Christou, G. *Inorg. Chem.* **1991**, *30*, 300.
(22) Randall, C. R.; Armstrong, W. H. *J. Chem. Soc., Chem. Commun.* **1988**, 986.
(23) Cramer, S. P. Biochemical Applications of X-ray Absorption Spectroscopy. In *Extended X-ray Absorption Fine Structure*; Konigsberger, D., Prins, R., Eds.; Plenum: New York, 1988; p 257.
(24) Money, J. K.; Folting, K.; Huffman, J. C.; Christou, G. *Inorg. Chem.* **1987**, *26*, 944.

S0020-1669(97)00113-4 CCC: $14.00

sulfur environment.[25−28] To this end, we recently reported the reactivities of Mo═O_t terminal bonds of a *cis*-dioxo precursor compound, [$MoO_2L(CH_3OH)$], containing a hetero donor (ONS) tridentate ligand, *viz.* *S*-methyl 3-((2-hydroxyphenyl)methyl)-dithiocarbazate (H_2L), that successfully models the turnover of oxidoreductase Mo enzymes.[29] As an extension of this work, we have used this tridentate ligand to study oxovanadium chemistry in donor environments partially occupied by sulfur.[30] Tridentate ligands are of intrinsic interest here because of their ability to form a VOL oxovanadium core with at least one coordination site available for accepting an additional ligand. This offers a strategic route for the synthesis of dinuclear mixed-valence oxovanadium(IV/V) compounds from the mononuclear counterparts with the use of potential bridging molecules as ancillary ligands. Herein we report the synthesis of mononuclear oxovanadium(V) and -(IV) complexes and their use as precursors to generate a (μ-oxo) dinuclear oxovanadium(IV/V) species. Crystal and molecular structures, magnetism, EPR, ^{1}H NMR, and electronic spectroscopies, and electrochemical properties are examined. Electron delocalization in the mixed-oxidation-state compound both in solution and in the solid state is also discussed.

Experimental Section

All the reactions were carried out under purified dinitrogen unless otherwise stated. Solvents were of reagent grade and were dried from appropriate reagents[31] and distilled under nitrogen prior to use. The tridentate ligand (H_2L)[30] and [$VO(acac)_2$][32] (Hacac = acetylacetone) were prepared according to published procedures.

Syntheses. [VOL(OMe)], 1a. Stoichiometric amounts of [$VO(acac)_2$] (0.4 g, 1.5 mmol) and the ligand H_2L (0.34 g, 1.5 mmol) were dissolved in 20 mL of methanol. The solution was heated under reflux in air for 2 h and cooled to room temperature. The solid that formed was filtered off, washed with methanol, and dried *in vacuo*. The crude product upon recrystallization from benzene under slow evaporation at room temperature gave shining dark brown crystals, which were filtered off and washed with petroleum ether (bp 40−60 °C). Yield: 0.23 g (46%). Anal. Calcd for $VC_{10}H_{11}N_2O_3S_2$: C, 37.27; H, 3.41; N, 8.69. Found: C, 37.3; H, 3.5; N, 8.8. IR (KBr pellet), cm^{-1}: ν(C⋯N), 1600 s; ν(C−O/phenolate), 1540 s; ν(V═O), 990 s; ν(C−S), 650 m. ^{1}H NMR ($CDCl_3$, 25 °C), δ/ppm, multiplicity, integration (assignment): 9.1, s, 1H (azomethyne); 7.7, m, 2H, and 7.3, m, 2H (aromatic ring); 5.3, s, 3H (methoxy); 2.7, s, 3H (SCH_3)

[VOL(OEt)], 1b. This compound was prepared by following the same procedure as described for **1a** using ethyl alcohol as solvent. Yield: 40%. Anal. Calcd for $VC_{11}H_{13}N_2O_3S_2$: C, 39.28; H, 3.87; N, 8.33. Found: C, 39.1; H, 3.7; N, 8.2. IR (KBr pellet), cm^{-1}: ν(C⋯N), 1595 s; ν(C−O/phenolate), 1540 s; ν(V═O), 995 s; ν(C−S), 650 m. ^{1}H NMR ($CDCl_3$, 25 °C), δ/ppm, multiplicity, integration (assignment): 9.0, s, 1H (azomethyne); 7.5, m, 2H, and 7.2, m, 2H (aromatic ring); 5.4, q, 2H (methylene); 2.65, s, 3H (SCH_3); 1.6, t, 3H (methyl).

[VOL(OPr^i)], 1c. This compound was also prepared similarly to **1a** using a 2-propanol and CH_2Cl_2 (1:1 v/v) mixture as solvent. The crude product was recrystallized from benzene. Yield: 42%. Anal. Calcd for $VC_{12}H_{15}N_2O_3S_2$: C, 41.14; H, 4.28; N, 8.0. Found: C, 41.5; H, 4.3; N, 8.0. IR (KBr pellet), cm^{-1}: ν(C⋯N), 1600 s; ν(C−O/phenolate), 1545 s; ν(V═O), 990 s; ν(C−S), 650 m.

[VOL(Im)], 2a. A mixture of [$VO(acac)_2$] (0.4 g, 1.5 mmol) and the ligand H_2L (0.34 g, 1.5 mmol) in acetonitrile (30 mL) and imidazole (Im) (0.11 g, 1.6 mmol) were heated under reflux for 1 h. The resulting brown-green solution was allowed to stand at room temperature overnight. Dark green crystals were collected by filtration, washed with Et_2O (4 × 10 mL), and dried *in vacuo*. Yield: 0.45 g (84%). Anal. Calcd for $VC_{12}H_{12}N_4O_2S_2$: C, 40.11; H, 3.34; N, 15.60. Found: C, 40.2; H, 3.1; N, 15.4. IR (KBr pellet), cm^{-1}: ν(N−H), 3200 b; ν(C⋯N), 1600 s; ν(C−O/phenolate), 1550 s; ν(V═O), 965 s. μ_{eff}(solid, 25 °C): 1.81 μ_B.

[VOL(BzIm)], 2b. This compound was obtained in 85% yield as dark green crystals by following the procedure described for **2a**, except that benzimidazole (BzIm) was used instead of imidazole. Anal. Calcd for $VC_{16}H_{14}N_4O_2S_2$: C, 46.94; H, 3.42; N, 13.69. Found: C, 46.5; H, 3.3; N, 13.3. IR (KBr pellet), cm^{-1}: ν(N−H), 3200 b; ν(C⋯N), 1600 s; ν(C−O/phenolate), 1540 s; ν(V═O), 960 s. μ_{eff}(solid, 25 °C): 1.82 μ_B.

(BzImH)[(LOV)$_2$O], 3. To a stirred suspension of **2b** (0.2 g, 0.5 mmol) in acetonitrile (20 mL) was added an equimolar amount of **1a**. Stirring was continued for *ca*. 2 h, during which a clear green solution appeared. It was filtered, and the filtrate was cooled to 0 °C, whereupon dark green crystals of compound **3** deposited overnight. The product was collected, washed with Et_2O, and dried *in vacuo*. The compound was sufficiently pure at this stage. Yield: 0.1 g (30%). Attempts to recrystallize it from an acetone/hexane mixture resulted in poor yields due to breakdown of the product. Anal. Calcd for $V_2C_{25}H_{23}N_6O_5S_4$: C, 41.84; H, 3.20; N, 11.71. Found: C, 41.5; H, 3.1; N, 11.2. IR (KBr pellet), cm^{-1}: ν(N−H), 3180 m; ν(C⋯N), 1600 s; ν(C−O/phenolate), 1545 s; ν(V═O), 980 s; ν_{asym}(V−O−V), 830 m. μ_{eff}(solid, 25 °C): 1.68 μ_B.

Physical Measurements. Electronic spectra in the near-IR region were recorded on a Hitachi U-3400 UV/vis/near-IR spectrophotometer. The X-band EPR spectra in solution at variable temperatures were recorded on a Bruker model ESP 300E spectrometer. A Varian model EM-360 spectrometer was used to acquire the ^{1}H NMR spectra. Room-temperature magnetic moments and IR and UV−vis spectra were obtained as described elsewhere.[33] Elemental analyses for C, H, and N were carried out in this laboratory (IACS) with a Perkin-Elmer 2400 analyzer.

Electrochemical measurements were performed at room temperature in an electrochemical cell (15 mL volume) fitted with a platinum working electrode, a platinum wire counter electrode, a saturated calomel reference electrode (SCE), and an inert-gas inlet. Dry degassed solvents containing 0.1 M NEt_4ClO_4 as the background electrolyte were used during the measurements. Bulk electrolyses were performed with the use of a Pt-gauze working electrode. The apparatus was a PAR model 362 scanning potentiostat. The ferrocene/ferrocenium (Fc/Fc^+) couple was used as the internal standard.[34]

X-ray Crystallography. (a) [VOL(OMe)], 1a. Diffraction-quality crystals of **1a** were obtained from a CH_2Cl_2 solution by slow evaporation. Intensity data for a dark brown block (0.24 × 0.32 × 0.42 mm) were measured at room temperature (20 °C) on a Rigaku AFC 6R diffractometer using graphite-monochromatized Mo Kα radiation, λ = 0.7107 Å; the $\omega-2\theta$ scan technique was employed to measure 4961 data (4701 unique) such that $2\theta_{max}$ was 55.0°. No decomposition of the crystal occurred during the data collection, and 3631 absorption-corrected (range of transmission factors: 0.674−1) data[35] which satisfied the $I \geq 3.0\sigma(I)$ criterion were used in the subsequent analyses. Crystal data are given in Table 1.

The structure was solved by direct methods[36] and refined by a conventional full-matrix least-squares procedure based on F.[37] Non-hydrogen atoms were refined with anisotropic displacement parameters,

(25) Dutta, S. K.; Kumar, S. B.; Bhattacharyya, S.; Chaudhury, M. *J. Chem. Soc., Dalton Trans*. **1994**, 97
(26) Kumar, S. B.; Chaudhury, M. *J. Chem. Soc., Dalton Trans*. **1990**, 2169.
(27) Chaudhury, M. *Inorg. Chem.* **1985**, *24*, 3011.
(28) Chaudhury, M. *Inorg. Chem.* **1984**, *23*, 4434.
(29) Dutta, S. K.; McConville, D. B.; Youngs, W. J.; Chaudhury, M. *Inorg. Chem.* **1997**, *36*, 2517.
(30) Dutta S. K.; Tiekink, E. R. T.; Chaudhury, M. *Polyhedron* **1997**, *16*, 1863.
(31) Perrin, D. D.; Armarego, W. L. F.; Perrin, D. R. *Purification of Laboratory Chemicals*, 2nd ed.; Pergamon: Oxford, England, 1980.
(32) Rowe, R. A.; Jones, M. M. *Inorg. Synth*. **1957**, *5*, 113.
(33) Bhattacharyya, S.; Kumar, S. B.; Dutta, S. K.; Tiekink, E. R. T.; Chaudhury, M. *Inorg. Chem.* **1996**, *35*, 1967.
(34) Gagné, R. R.; Koval, C. A.; Lisensky, G. C. *Inorg. Chem*. **1980**, *19*, 3854.
(35) Walker, N.; Stuart, D. *Acta Crystallogr*. **1983**, *A39*, 158.
(36) Sheldrick, G. M. *SHELXS86: Program for the automatic solution of crystal structure*; University of Göttingen: Göttingen, Germany, 1986.
(37) *teXsan: Structure Analysis Package*; Molecular Structure Corp.: The Woodlands, TX, 1992.

Table 1. Summary of Crystallographic Data

empirical formula	$C_{10}H_{11}N_2O_3S_2V$	$C_{25}H_{23}N_6O_5S_4V_2$
fw	322.3	715.6
space group	triclinic, $P\bar{1}$ (No. 2)	monoclinic, $P2_1/n$ (No. 14)
a, Å	11.045(1)	10.10(1)
b, Å	13.429(4)	20.594(9)
c, Å	9.611(3)	14.679(8)
α, deg	100.00(1)	90
β, deg	114.33(1)	95.28(6)
γ, deg	81.00(1)	90
V, Å^3	1273.4(5)	3041(3)
Z	4	4
T, K	293	293
λ(Mo Kα), Å	0.7107	0.7107
ρ_{calcd}, g cm^{-3}	1.681	1.567
μ, cm^{-1}	9.47	9.35
R^a ($R_w{}^b$)	0.039 (0.043)	0.072 (0.066)

^{a} $R = \sum||F_o| - |F_c||/\sum|F_o|$. ^{b} $R_w = \sum[(|F_o| - |F_c|)w^{1/2}]/\sum[|F_o|w^{1/2}]$.

and hydrogen atoms were included in the model at their calculated positions (C−H = 0.97 Å). At convergence [σ weights, i.e. $1/\sigma^2(F)$], $R = 0.039$ and $R_w = 0.043$; final refinement details are given in Table 1. The maximum peak in the final difference map was 0.34 e Å^{-3}. Scattering factors for all atoms were those incorporated in the teXsan program.[37] The crystallographic numbering scheme is shown in Figure 1, which was drawn with the ORTEP program[38] using 25% probability ellipsoids.

(b) (BzImH)[(LOV)$_2$O], 3. Crystals of **3** were grown at room temperature by slow diffusion of *n*-hexane into an acetone solution of the complex. Data collection and reduction and structure solution and refinement were as above for a dark green crystal 0.11 × 0.16 × 0.29 mm. Of the 7630 data measured ($2\theta_{max}$ was 50.0°), 7239 were unique, and of these, 2068 absorption-corrected data (minimum and maximum transmission factors: 0.644, 1) satisfied the $I \geq 3.0\sigma(I)$ criterion; $R = 0.072$ and $R_w = 0.066$. The maximum peak in the final difference map was 0.66 e Å^{-3}, and the ORTEP diagram was drawn at the 30% probability level. As can be seen from this diagram (Figure 2), there are indications of disorder in the structure, reflecting the limited data set obtained. Although precise geometric information is lacking for the ligand atom parameters in particular, the gross/chemical features of the structure were determined unambiguously. Relevant crystallographic data are given in Table 1.

Results and Discussion

Synthesis. The oxoalkoxyvanadium(V) compounds [VOL(OR)] (**1a**−**c**) are obtained in *ca*. 40% yield by refluxing in air stoichiometric amounts (1:1 mole ratio) of [VO(acac)$_2$] and the tridentate ONS ligand [H$_2$L] in the appropriate alcohol as solvent. During this reaction, vanadium is oxidized from its initial +IV state, underscoring the ability of alkoxy group to stabilize high oxidation states.[39] On the other hand, when this reaction is carried out in acetonitrile under nitrogen in the presence of a heterocyclic base (B), the product is the oxovanadium(IV) complex [VOLB] (B: Im, **2a**; BzIm, **2b**).

These mononuclear complexes are subsequently used as precursors to generate dinuclear mixed-oxidation-state compound by following the synthetic route outlined in Scheme 1. The product obtained is a (μ-oxo)divanadium(IV,V) complex anion, stabilized by a protonated benzimidazole counterion (**3**) as confirmed by X-ray crystallography (*vide infra*). A trace of moisture is probably the source of the proton here that initiates the formation of an oxo-bridged dimer with a stable $(V_2O_3)^{3+}$ core, found to be present in all of the dinuclear vanadium(IV/V) compounds characterized so far by X-ray crystallography.[40−44] Compound **3** is a brown-green crystalline solid, obtained in *ca*. 30% yield.

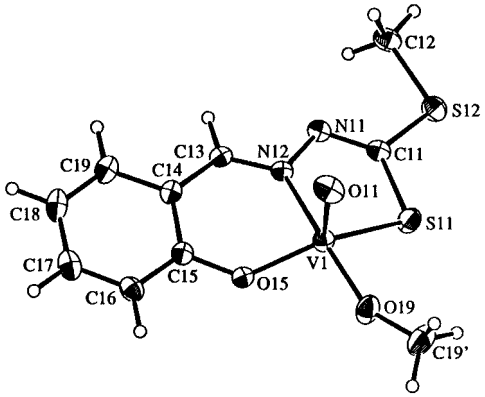

Figure 1. Molecular structure and atom-numbering scheme of one of the two crystallographically independent molecules of [VOL(OMe)] (**1a**) with 25% probability ellipsoids.

Scheme 1

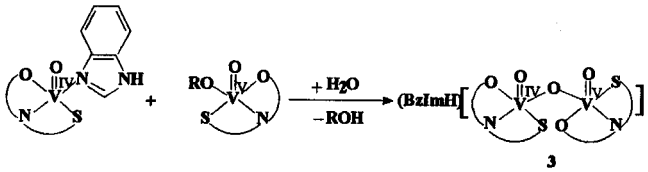

The IR spectra of the complexes show features that are characteristic of the tridentate ONS mode of coordination of the ligand in the thioenol form.[29,30] In addition, the compounds exhibit a strong band in the 995−960 cm^{-1} range due to the terminal V=O stretching, along with a broad medium-intensity band in the high-frequency region (3200 cm^{-1} for **2a**,**b** and 3180 cm^{-1} for **3**), associated with the N−H stretch of the heterocyclic ring. A characteristic feature in the form of a prominent band near 830 cm^{-1} is also observed for the dinuclear complex (**3**) due to V−O−V asymmetric bridge vibrations.

The ^{1}H NMR spectra of the free ligand H$_2$L and its oxovanadium(V) complexes **1a**,**b** were recorded in CDCl$_3$. The free ligand displays two characteristic resonances, one with a sharp feature at 10.9 ppm and the other with a broad peak at 3.0 ppm due to phenolic OH and NH functionalities, respectively, which are missing in the spectra of the complexes. These indicate that the coordinated ligand is dianionic. Besides having all the remaining peaks of the coordinated ONS ligand, the spectrum of **1b** displays a quartet at 5.4 ppm ($J = 7.3$ Hz) and a triplet at 1.6 ppm ($J = 7.0$ Hz) due to the methylene and methyl protons, respectively, of the coordinated ethoxy group. Similar resonances with expected splitting patterns are also obtained with **1a** (see Experimental Section).

Description of Crystal Structures. The molecular structure of [VOL(OMe)] is shown in Figure 1, and selected interatomic parameters are listed in Table 2. The asymmetric unit of **1a** contains two independent molecules; however, there are only minor conformational differences between them. The unit cell comprises four molecules, and the shortest non-hydrogen intermolecular contact occurs between the N(21) and C(13)′

(38) Johnson, C. K. *ORTEP II*; Report ORNL 5136; Oak Ridge National Laboratory: Oak Ridge, TN, 1976.
(39) Kessissoglou, D. P.; Butler, W. M.; Pecoraro, V. L. *J. Chem. Soc., Chem. Commun*. **1986**, 1253.
(40) Nishizawa, M.; Hirotsu, K.; Ooi, S.; Saito, K. *J. Chem. Soc., Chem. Commun*. **1979**, 707.
(41) Kojima, A.; Okajaki, K.; Ooi, S.; Saito, K. *Inorg. Chem*. **1983**, *22*, 1168.
(42) Launay, J.-P.; Jeannin, Y.; Daoudi, M. *Inorg. Chem*. **1985**, *24*, 1052.
(43) Schulz, D.; Weyhermuller, T.; Wieghardt, K.; Nuber, B. *Inorg. Chim. Acta* **1995**, *240*, 217.
(44) Pessoa, J. C.; Silva, J. A. L.; Vieira, A. L.; Vilas-Boas, L.; O'Brien, P.; Thronton, P. *J. Chem. Soc., Dalton Trans*. **1992**, 1745.

Table 2. Selected Bond Distances and Angles for [VOL(OMe)] (**1a**)

	Distances (Å)		
V(1)−S(11)	2.318(1)	V(2)−S(21)	2.328(1)
V(1)−O(11)	1.563(3)	V(2)−O(21)	1.564(3)
V(1)−O(15)	1.804(2)	V(2)−O(25)	1.819(2)
V(1)−O(19)	1.723(3)	V(2)−O(29)	1.724(3)
V(1)−N(12)	2.104(3)	V(2)−N(22)	2.089(3)
N(11)−N(12)	1.380(4)	N(21)−N(22)	1.388(4)
N(11)−C(11)	1.277(4)	N(21)−C(21)	1.273(4)
N(12)−C(13)	1.281(4)	N(22)−C(23)	1.289(4)
	Angles (deg)		
S(11)−V(1)−O(11)	108.2(1)	S(21)−V(2)−O(21)	107.7(1)
S(11)−V(1)−O(15)	136.72(9)	S(21)−V(2)−O(25)	141.23(9)
S(11)−V(1)−O(19)	85.19(9)	S(21)−V(2)−O(29)	84.79(9)
S(11)−V(1)−N(12)	77.50(8)	S(21)−V(2)−N(22)	77.68(8)
O(11)−V(1)−O(15)	111.4(1)	O(21)−V(2)−O(25)	117.7(1)
O(11)−V(1)−O(19)	107.8(2)	O(21)−V(2)−O(29)	106.3(2)
O(11)−V(1)−N(12)	93.2(1)	O(21)−V(2)−N(22)	95.3(1)
O(15)−V(1)−O(19)	98.6(1)	O(25)−V(2)−O(29)	100.1(1)
O(15)−V(1)−N(12)	83.4(1)	O(25)−V(2)−N(22)	83.7(1)
O(19)−V(1)−N(12)	156.2(1)	O(29)−V(2)−N(22)	155.5(1)

atoms of 3.125(4) Å (symmetry operation: $1 + x, y, z$). The vanadium atom in each molecule is five-coordinate, existing in a distorted square pyramidal geometry in which the basal plane is defined by S, N, and O atoms, derived from the tridentate ligand, and the O atom of the methoxide; the apical position is occupied by the oxo group.[45] The deviations from the least-squares plane through the S(11), O(15), O(19), and N(12) atoms comprising the square plane are −0.035(1), −0.191(3), 0.318(4), and 0.192(3) Å, respectively, and the V(1) atom lies 0.5966(7) Å above this plane in the direction of the O(11) atom; comparable values for the second molecule are −0.024(1), −0.146(3), 0.252(4), and 0.158(3) Å, respectively with the V(2) atom lying 0.5502(7) Å out of the plane. The greatest distortion from ideal geometry is manifested in the S(11)−V(1)−O(15) angle of 136.72(9)° [141.23(9)°], which arises as a result of the restricted bite angle of the tridentate ligand.

The coordination mode of the tridentate ligand leads to the formation of both five- and six-membered rings. The relatively short C(11)−N(11) and C(13)−N(12) bond distances of 1.277(4) and 1.281(4) Å, respectively [1.273(4) and 1.289(4) Å for the second molecule], coupled with the N(11)−N(12) distance of 1.380(4) Å [1.388(4) Å], indicate that there is conjugation along the backbone of the tridentate ligand; the value of the C(11)/N(11)/N(12)/C(13) torsion angle is 171.4(3)° [175.2(3)°].

The crystal structure of (BzImH)[(LOV)$_2$O], **3**, features an oxo-bridged dinuclear oxovanadium(IV/V) monoanion and a bezimidazolium (BzImH) cation as shown in Figure 2; the nature of the intermolecular contacts confirms the presence of hydrogen atoms on each of the nitrogen atoms of benzimidazole (see below), thus indicating the cationic nature of the heterocyclic base. Each vanadium center is coordinated by the dinegative L *via* a S, N, and O donor set, a terminal oxo group, and a bridging oxygen atom, O(2), leading to a five-coordination geometry. Selected bond lengths and angles are listed in Table 3. For V(1), the mean deviation of the S, N, O(2), and O(7) atoms from their least-squares plane is 0.110 Å [0.092 Å for V(2)], and the V(1) atom lies 0.546(2) Å [0.596(2) Å] out of this plane in the direction of the O(1) atom.

The molecule does not have crystallographically imposed symmetry. Unlike many other oxo-bridged divanadium(IV,V) complexes, **3** is a bent molecule with a V−O−V bridge angle far removed from linearity. To our knowledge, the observed

(45) An alternate description of the coordination geometry would be one based on a distorted trigonal bipyramid with the axial positions being occupied by the O(19) and N(12) atoms.

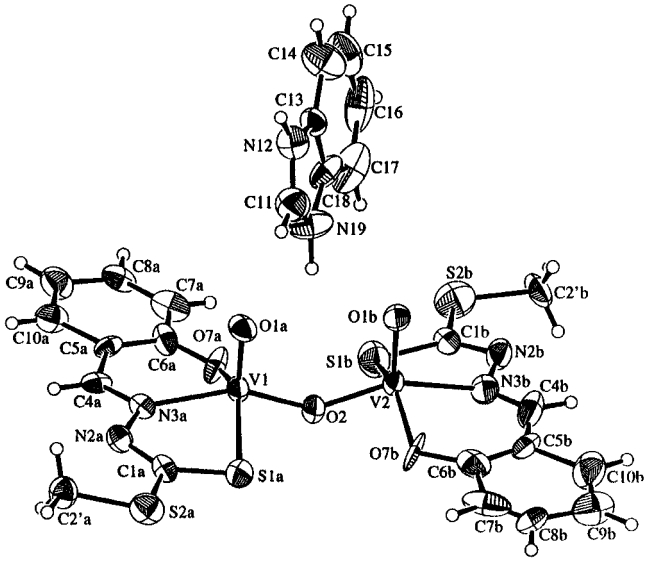

Figure 2. Molecular structure and atom-numbering scheme for (BzImH)[(LOV)$_2$O] (**3**). The ellipsoids represent a 30% probability.

Table 3. Selected Bond Distances and Angles for (BzImH)[(LOV)$_2$O] (**3**)

	Distances (Å)		
V(1)−S(1a)	2.361(4)	V(2)−S(1b)	2.359(5)
V(1)−O(1a)	1.582(7)	V(2)−O(1b)	1. 584(7)
V(1)−O(2)	1.768(7)	V(2)−O(2)	1.833(7)
V(1)−O(7a)	1.880(9)	V(2)−O(7b)	2.080(9)
V(1)−N(3a)	2.13(1)	V(2)−N(3b)	2.12(1)
S(1a)−C(1a)	1.71(1)	S(1b)−C(1b)	1.68(1)
	Angles (deg)		
S(1a)−V(1)−O(1a)	107.5(3)	S(1b)−V(2)−O(1b)	106.3(3)
S(1a)−V(1)−O(2)	88.6(2)	S(1b)−V(2)−O(2)	86.1(3)
S(1a)−V(1)−O(7a)	142.6(3)	S(1b)−V(2)−O(7b)	144.8(3)
S(1a)−V(1)−N(3a)	77.4(3)	S(1b)−V(2)−N(3b)	81.0(5)
O(1a)−V(1)−O(2)	107.8 (3)	O(1b)−V(2)−O(2)	107.8(4)
O(1a)−V(1)−O(7a)	107.8 (4)	O(1b)−V(2)−O(7b)	108.6 (4)
O(1a)−V(1)−N(3a)	97.7(4)	O(1b)−V(2)−N(3b)	100.7 (4)
O(2)−V(1)−O(7a)	92.1(4)	O(2)−V(2)−O(7b)	87.1(3)
O(2)−V(1)−N(3a)	153.8(4)	O(2)−V(2)−N(3b)	151.1(4)
O(7a)−V(1)−N(3a)	85.7(4)	O(7b)−V(2)−N(3b)	88.7(5)
	V(1)−O(2)−V(2) 144.0(6)		

Hydrogen Bond Geometry

D−H···A	H···A, Å	D···A, Å	D−H···A, deg
N(12)′−H(12)′···O(7b)[a]	2.12	3.05(1)	169
N(12)′−H(12)′···O(1b)[a]	2.87	3.26(2)	106
N(19)−H(19)···O(1b)	2.82	3.15(2)	102

[a] Atoms are related by the symmetry operation $1 - x, -y, 1 - z$.

bridge angle of 144.0(6)° is the smallest among those of similar complexes for which crystal structures are known (summarized in Table 4). Of particular interest is the presence of a rarely observed[44] *syn*-dioxo−μ-oxo $(V_2O_3)^{3+}$ core in **3** in contrast to the thermodynamically more stable *anti* configuration[46] (Table 4). The stability of the bent *syn*-dioxo core in the present case can be associated with the presence of the $BzImH^+$ cation, which leads to packing of the $(V_2O_3)^{3+}$ core in a bent form. As can be seen from Table 3, there are also some hydrogen-bonding interactions that hold the counterions together in **3**. The most significant hydrogen-bonding contact in the lattice which is intermolecular in nature (Figure S1, Supporting Information) involves the H(12) atom such that the distances O(7b)···H(12)′ and O(1b)···H(12)′ are 2.12 and 2.87 Å, respectively. The H(19) atom of the BzImH cation forms a weak contact with the O(1b) atom, with O(1b)···H(19) being 2.82 Å.

(46) Young, C. G. *Coord. Chem. Rev.* **1989**, *96*, 89.

Table 4. Compilation of Relevant Structural Data for Mixed-Valence Dinuclear μ-Oxo Vanadium(IV/V) Complexes Having a $(V_2O_3)^{3+}$ Core

complex[a]	V−O$_t$, Å	V−O$_b$, Å	V−O−V, deg	orientation of V=O$_t$ bonds	ref
$(NH_4)_3[V_2O_3(nta)_2]\cdot 3H_2O$	1.607	1.810	180	*anti*	40
$Na[V_2O_3(S\text{-peida})_2]\cdot NaClO_4\cdot H_2O$	1.622(4)	1.875(4)	179.5(3)	*anti*	41
	1.613(4)	1.763(4)			
$H[V_2O_3(pmida)_2]\cdot 4H_2O$	1.592(5)	1.79(2)	175.3(7)	*anti*	42
	1.620(8)	1.82(2)			
$[V_2O_3(L^1)_2]Br$	1.620(4)	1.825(1)	165.4(3)	*anti*	43
$[V_2O_3(L^2)_2]ClO_4\cdot 0.5$(acetone)	1.632(3)	1.716(3)	148.4(2)	*anti*	43
	1.605(3)	1.927(3)			
$Na[V_2O_3(\text{DL-salser})_2]\cdot 5H_2O$	1.589(6)	1.866(5)	146.6(2)	*syn*	44
	1.580(6)	1.754(6)			
$(BzImH)[V_2O_3(L)_2]$	1.582(7)	1.768(7)	144.0(6)	*syn*	this work
	1.584(7)	1.833(7)			

[a] nta^{3-} = nitrilotriacetate; *S*-peida^{2-} = (*S*)-[[1-(2-pyridyl)ethyl]imino]diacetate; pmida^{2-} = ((2-pyridylmethyl)imino)diacetate; $(L^1)^-$ = 1,4,7-triazacyclononane-*N*-acetate; HL^2 = 1-(2-hydroxybenzyl)-1,4,7-triazacyclononane; salser^{2-} = *N*-salicylideneserinate.

Compounds with a $V^{IV}-O-V^V$ bridge angle close to 180° have delocalized vanadium oxidation states,[40,42,43] the only exception being $H[V_2O_3(S\text{-peida})_2]\cdot NaClO_4\cdot H_2O$, which shows a trapped-valence configuration in the solid state as confirmed by X-ray crystallography.[41] The presence of a linear V−O−V structure can permit effective interactions between the d_{xy} orbitals of the participating vanadium nuclei *via* the $p\pi$ orbital of the bridging oxygen atom.[42,46] However, in the present case, as well as in some others,[43,44] substantial departures of the V−O−V bridge angles from linearity generate valence-trapped situations due to poor overlap of symmetry-constrained d_{xy} orbitals. This leads to differences in bond lengths around the vanadium centers, especially in the equatorial plane (Table 3), since the excess electron in V(IV) lies in a d_{xy} orbital, which is perpendicular to the metal−terminal oxygen bond axis. Thus the equatorial V(1)−O(7a) bond distance [1.880(9) Å] differs significantly from the corresponding bond distance V(2)−O(7b) [2.080(9) Å], associated with the second vanadium center. The inequivalance is also seen in the bridging V−O distances; e.g., V(1)−O(2) = 1.768(7) Å as compared to V(2)−O(2) = 1.833(7) Å. Considering the smaller ionic radius of vanadium(V), the observed bond lengths indicate valence localization in the compound with V(1) and V(2) being vanadium(V) and -(IV), respectively. As revealed from Table 3, a similar trend is not followed with the remaining equatorial distances in **3**. This is, however, not quite unexpected, considering the strong *trans*-labilizing influences of the shorter V(1)−O(2) and V(1)−O(7a) distances, which offset the opposing influence due to the greater Lewis acidity of V(1). As a result, the remaining equatorial distances V(1)−N(3a) and V(1)−S(1a) are almost identical to the corresponding distances involving the V(2) atom.

Magnetic Susceptibility and EPR Spectra. At room temperature, polycrystalline samples of oxovanadium(IV) complexes have molar magnetic moments of 1.81 (**2a**) and 1.82 μ_B (**2b**), in agreement with the spin-only value for a formally d^1 system. As expected, mixed-valence dinuclear complex **3** also has a close to normal magnetic moment of 1.68 μ_B at 298 K.

The X-band EPR spectra of the oxovanadium(IV) complexes **2a**,**b** are grossly identical. At room temperature in a DMF/toluene (1:10 v/v) solution, a typical eight-line spectral pattern is obtained at $\langle g\rangle = 2.00$ with $\langle A\rangle = 89 \times 10^{-4}$ cm^{-1}. EPR spectra of the mixed-valence compound **3** were measured in fluid as well as in frozen acetonitrile solution and are shown in Figure 3. At ambient temperature, an isotropic pattern is obtained with 15 vanadium hyperfine lines (Figure 3a) in the $g = 2$ region, which indicates that the excess electron is delocalized between the participating metal centers. The hyperfine splitting parameter $\langle A\rangle_{15}$ is 44×10^{-4} cm^{-1}. The

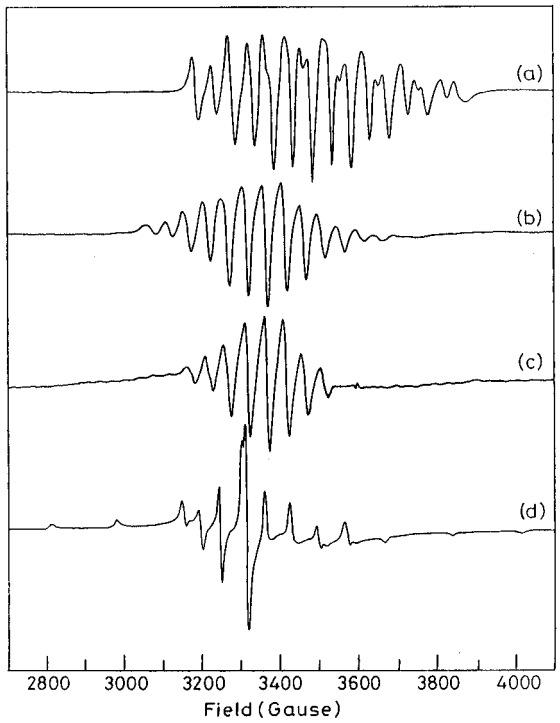

Figure 3. X-Band EPR spectra of (BzImH)[(LOV)$_2$O] (**3**) in acetonitrile: (a) 298 K; (b) 235 K; (c) 225 K; (d) 80 K.

observation of a 15-line profile, according to Robin and Day,[47] would suggest a class II or III character for this compound on the EPR time scale (*ca* 10^{-9} s).[48−50] In the frozen solution (80 K), however, **3** exhibits an anisotropic spectrum with axial features (Figure 3d), typical of mononuclear vanadium(IV) complexes,[9,30] with $g_{\|} = 1.963$ ($A_{\|} = 157 \times 10^{-4}$ cm^{-1}) and $g_{\perp} = 1.994$ ($A_{\perp} = 54 \times 10^{-4}$ cm^{-1}). This indicates that the species is valence-trapped at this temperature. In order to locate the temperature at which spectral coalescence takes place, variable-temperature EPR spectra of the compound were measured.[51] As shown in Figure 3b, the 15-line pattern continues to be observed at 235 K. Transformation of the 15-line to an 8-line profile occurs at *ca.* 225 K (Figure 3c), where the solution still retains its fluidity. An estimate of the activation energy ($E_{th}^{\ddagger}$) and the thermal electron transfer rate (k_{th}) can be

(47) Robin, M. B.; Day, P. *Adv. Inorg. Chem. Radiochem.* **1967**, *10*, 247.
(48) Heitner-Wirguin, C.; Selbin, J. *J. Inorg. Nucl. Chem.* **1968**, *30*, 3181.
(49) Babonneau, F.; Sanchez, C.; Livage, J.; Launay, J.-P.; Daoudi, M.; Jeannin, Y. *Nouv. J. Chim.* **1982**, *6*, 353.
(50) Dutta, S.; Basu, P.; Chakravorty, A. *Inorg. Chem.* **1993**, *32*, 5343.
(51) Gagné, R. R.; Kovac, C. A.; Smith, T. J.; Cimolino, M. C. *J. Am. Chem. Soc.* **1979**, *101*, 4571.

Table 5. Summary of Electronic Spectral Data[a]

complex	λ_{max}, nm (ϵ_{max}, M^{-1} cm^{-1})
1a	400 (8600), 307 (27 600), 238 (26 400)
1b	400 (7900), 307 (27 800), 237 (26 700)
1c	400 (7050), 308 (27 900), 237 (26 500)
2a	712 (55), 529 (100), 393 (9300), 286 (21 900)
2b	720 (70), 536 (120), 395 (8000), 298 (24 700)
3	970 (1670), 740 (sh, 900), 390 (14 800), 298 (36 500)

[a] Spectra of compounds **1a**−**c** were recorded in CH_2Cl_2, those of **2a**,**b** were recorded in DMF, and that of **3** was recorded in CH_3CN

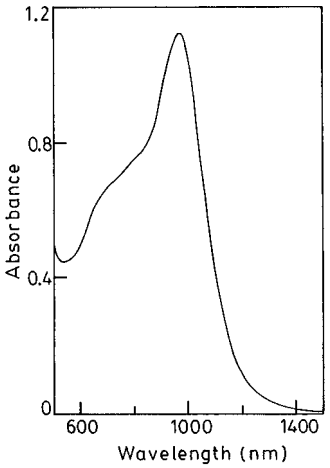

Figure 4. Electronic absorption spectrum of (BzImH)[(LOV)$_2$O] (**3**) in acetonitrile (concentration 6.7×10^{-4} M).

made[51,52] by using eq 1, in which the symbols have their usual

$$k_{th} = (kT/h)\exp(-E_{th}^{\ddagger}/RT) \quad (1)$$

significance.[53] Following an approximation considered by Gagné and co-workers[51] that the EPR lifetime (5.5×10^8 s^{-1}) is equal to k_{th} at the coalescence temperature, $E_{th}^{\ddagger}$ and k_{th} are estimated to be approximately 4 kcal mol^{-1} and 7.3×10^9 s^{-1} (at 298 K), respectively.

Electronic Spectra. The electronic absorption spectra of the complexes are summarized in Table 5. The mononuclear complexes **1a**−**c** (in CH_2Cl_2) and **2a**,**b** (in DMF) exhibit an intense $PhO^- \rightarrow V(d\pi)$ LMCT band at *ca.* 400 nm, which shows some dependence on the substituent present in the *para* position of the phenolate ring.[30] Complexes **2a**,**b** also show two additional bands of moderate intensity (ϵ_{max} 55−120 M^{-1} cm^{-1}) at *ca.* 720 and 530 nm due to the ligand-field transitions $d_{xy} \rightarrow d_{xz}$, d_{yz} and $d_{xy} \rightarrow d_{x^2-y^2}$, respectively, for the oxovanadium(IV) chromophore.[54] A third d−d band expected at higher energy due to a $d_{xy} \rightarrow d_{z^2}$ transition is probably obscured by the tail of the LMCT absorption.

The electronic spectrum of the mixed-valence complex **3** in acetonitrile exhibits several prominent features (Table 5) which include a strong LMCT band (ϵ_{max} 14 800 M^{-1} cm^{-1}) at 390 nm due to a $PhO^- \rightarrow V(d\pi)$ transition, as observed with the mononuclear complexes. Additionally, there is a broad shoulder (ϵ_{max} 900 M^{-1} cm^{-1}) centered at *ca.* 740 nm, comprising more than one ligand-field transition. The most important feature of the spectrum is the occurrence of a broad peak in the near-IR region at 970 nm (Figure 4). The spectral width at half-height ($\Delta\nu_{1/2}$) and the intensity (ϵ_{max} 1670 M^{-1} cm^{-1}) suggest it to be an intervalence transfer (IT) transition. For weakly interacting

Table 6. Summary of Electrochemical Data[a] for the Vanadium(V) Complexes

	V(V)/V(IV)			
complex	$E_{1/2}$,[b] V	ΔE_p,[c] mV	i_{pc}/i_{pa}	n[d]
1a	0.41	70	0.95	0.96
1b	0.40	75	0.90	0.98
1c	0.39	90	1.00	0.97

[a] Solvent CH_2Cl_2; supporting electrolyte NEt_4ClO_4 (0.1 M); solute concentration *ca.* 10^{-3} M; working electrode platinum. [b] Potentials are *vs* SCE and estimated by cyclic voltammetry at a scan rate of 50 mV s^{-1}; $E_{1/2} = 0.5(E_{pc} + E_{pa})$. [c] $\Delta E_p = E_{pc} - E_{pa}$. [d] Number of electrons per molecule, determined by controlled-potential coulometry.

mixed-valence systems (class II), Hush[55] proposed a relationship (eq 2) between $\Delta\nu_{1/2}$ and band energy (ν_{max}). For compound

$$\Delta\nu_{1/2} = (2310\nu_{max})^{1/2} \quad (2)$$

3, the observed bandwidth (∼2140 cm^{-1})[56] is *ca.* 50% narrower than the calculated value (4890 cm^{-1}). Moreover, no solvent dependence of the IT band is observed in this case. For example, the band appears at 965 nm in acetone and at 970 nm in DMF. These observations are at variance with the behavior expected for a weakly interacting system. Indeed, the degree of electron coupling (H_{AB}) between the vanadium centers in **3** as obtained from eq 3 is 2210 cm^{-1} (V···V distance $r = 3.426$ Å), indicating fairly strong delocalization of the extra electron.[57]

$$H_{AB} = [2.05 \times 10^{-2}(\epsilon_{max}(\Delta\nu_{1/2})\nu_{max})^{1/2}]/r \quad (3)$$

Electrochemistry. Cyclic voltammograms of the mononuclear vanadium(V) complexes (**1a**−**c**) in CH_2Cl_2 solution (containing 0.1 M NEt_4ClO_4 as supporting electrolyte at a platinum working electrode) have identical features due to a reduction process ($E_{1/2} \sim 0.40$ V *vs* SCE) corresponding to a V(V)/V(IV) electron transfer. The free ligand is electroinactive in the potential range −1.0 to +1.0 V (*vs* SCE). The couple exhibits the usual features of Nernstian reversibility (*i.e.*, $i_{pc}/i_{pa} \approx 1.0$, $i_p/v^{1/2}$ remaining independent of scan rate in the range 50−500 mV s^{-1}). The peak potential separations (ΔE_p) are in the range 70−90 mV (Table 6) at a scan rate of 50 mV s^{-1} and are comparable to that of the ferrocenium/ferrocene couple (85 mV) under the same experimental conditions, indicating that the observed voltammogram defines a one-electron process (eq 4). The single-electron stoichiometry of this process was further

$$[V^{V}OL(OR)]^0 \overset{+e^-}{\rightleftharpoons} [V^{IV}OL(OR)]^- \quad (4)$$

confirmed by controlled-potential coulometric experiments ($n = 0.97 \pm 0.1$). For the mixed-valence compound **3**, a one-electron oxidation (eq 5) with $E_{1/2} = 0.42$ V and $\Delta E_p = 75$

$$[LOV^{V}-O-V^{IV}OL]^- \overset{-e^-}{\rightleftharpoons} [LOV^{V}-O-V^{V}OL]^0 \quad (5)$$

mV (which remains constant regardless of scan rate in the range 50−500 mV s^{-1}) is observed in acetonitrile solution. This and other observations ($i_{pa}/i_{pc} \approx 1.0$) indicate that this step is electrochemically reversible.[58] Oxidative controlled-potential electrolysis experiments with a platinum-gauze electrode (work-

(52) Long, R. C.; Hendrickson, D. N. *J. Am. Chem. Soc.* **1983**, *105*, 1513.
(53) Glasstone, S.; Laidler, K. J.; Eyring, H. *The Theory of Rate Processes*; McGraw-Hill: New York, 1941.
(54) Ballhausen, C. J.; Gray, H. B. *Inorg. Chem.* **1962**, *1*, 111.
(55) Hush, N. S. *Prog. Inorg. Chem.* **1967**, *8*, 391.
(56) $\Delta\nu_{1/2}$ was estimated from Figure 4 by Gaussian analysis of the spectrum using a locally developed least-squares program.
(57) Ward, M. D. *Chem. Soc. Rev.* **1995**, 121.
(58) Brown, E. R.; Large, R. F. Electrochemical Methods. In *Physical Methods in Chemistry*; Weissberger, A., Rossiter, B., Eds.; Wiley-Interscience: New York, 1971; Part IIA, Chapter VI.

ing potential 0.6 V) confirmed the above electron stoichiometry ($n = 1.0 \pm 0.1$).

Concluding Remarks

The (μ-oxo)divanadium(IV,V) complex **3** has a trapped-valence structure in the solid state as revealed from X-ray crystallographic analysis. The $(V_2O_3)^{3+}$ core has a rare *syn*-dioxo$-\mu$-oxo configuration with a V$-$O$-$V bridge angle of 144.0(6)°. The presence of the benzimidazolium counterion perhaps contributes to the stability of this unusual structure. EPR and electronic spectroscopic and cyclic voltammetric studies indicate that in **3** the oxo-bridged structure is retained in solution. The appearance of 15-line EPR spectrum indicates detrapping of the odd electron at room temperature in solution. Thus, one can find in **3** an interesting oxo-bridged divanadium(IV,V) moiety with a $(V_2O_3)^{3+}$ core that shows a trapped-valence structure in the solid state and becomes sufficiently delocalized in solution at room temperature.

Acknowledgment. Support of this work by the Council of Scientific and Industrial Research, New Delhi, is gratefully acknowledged. We express special thanks to Professor K. Nag for helpful discussions and to Professor A. K. Pal for making the near-IR spectrophotometer available to us. Financial support received from the Australian Research Council is also acknowledged.

Supporting Information Available: Figures S-1 and S-2, showing the unit cell contents for **1a** and **3** (2 pages). Two X-ray crystallographic files, in CIF format, are available on the Internet only. Ordering and access information is given on any current masthead page.

IC970113S